2007 International Conference in Honor of Claude Lobry

Generic analysis of the response of calcifying microalgae to an elevation of pCO_2 : qualitative *vs* quantitative analysis

Olivier Bernard*[a] — Antoine Sciandra[b]

[a] COMORE, INRIA
BP93,06 902 Sophia-Antipolis cedex

* Corresponding author
olivier.bernard@inria.fr

[b] LOV, UMR 7093
B.P. 28, 06234, Villefranche-sur-mer FRANCE
antoine.sciandra@obs-vlfr.fr

ABSTRACT. Calcifying microalgae can play a key role in atmospheric CO_2 trapping through large scale precipitation of calcium carbonate in the oceans. However, recent experiments revealed that the associated fluxes may be slow down by an increase in atmospheric CO_2 concentration. In this paper we design models to account for the decrease in calcification and photosynthesis rates observed after an increase of pCO_2 in *Emiliania huxleyi* chemostat cultures. Since the involved mechanisms are still not completely understood, we consider various models, each of them being based on a different hypothesis. These models are kept at a very general level, by maintaining the growth and calcification functions in a generic form, *i.e.* independent on the exact shape of these functions and on parameter values. The analysis is thus performed using these generic functions where the only hypothesis is an increase of these rates with respect to the regulating carbon species. As a result, each model responds differently to a pCO_2 elevation. Surprisingly, the only models whose behaviour are in agreement with the experimental results correspond to carbonate as the regulating species for photosynthesis. Finally we show that the models whose qualitative behaviour are wrong could be considered as acceptable on the basis of a quantitative prediction error criterion.

RÉSUMÉ. Les microalgues calcifiantes jouent un rôle clé dans le piégeage du CO_2 atmosphérique d'origine anthropique en précipitant du carbonate de calcium qui sédimente au fond des océans. Toutefois, des expériences en laboratoire ont suggéré que cette activité biologique pourrait être diminuée par l'augmentation de la pression partielle de CO_2 (pCO_2) dans les océans qui a tendance à s'équilibrer avec celle de l'atmosphère. Dans ce papier, nous concevons des modèles dynamiques pour essayer de simuler la diminution des taux de calcification et de photosynthèse observés chez *Emiliania huxleyi* après une hausse de la pCO_2 reproduite en chémostat. Comme les mécanismes physiologiques impliqués sont encore loin d'être complètement élucidés, nous considérons différents modèles, chacun d'eux étant basé sur une hypothèse biologique différente. Ces modèles, construits en utilisant des fonctions génériques pour caractériser les processus de croissance et de calcification, peuvent être analysés indépendamment de la forme exacte de ces fonctions et de la valeur des paramètres. L'étude s'appuie donc sur ces fonctions génériques où la seule hypothèse est une régulation de ces taux par une des trois formes qui composent la totalité du carbone inorganique dissous : le CO_2, les carbonates et les bicarbonates. Il s'en suit que chaque modèle réagit différemment à une élévation de la pCO_2. Contrairement aux hypothèses classiquement admises, notre étude montre que les seuls modèles dont le comportement est en accord avec les résultats expérimentaux sont

ceux pour lesquels une régulation de la photosynthèse par les carbonates a été supposée, ce qui corrobore les conclusions de travaux récents. Enfin, nous montrons que les modèles dont le comportement qualitatif est mauvais ne seraient pas rejetés sur la base d'un critère quantitatif d'erreur de prédiction.

KEYWORDS : coccolithophore, photosynthesis, calcification, multimodel, pCO_2, greenhouse effect, qualitative approach.

MOTS-CLÉS : Coccolithophoridés, photosynthèse, calcification, approche multimodèle, pCO_2 , effet de serre, approche qualitative.

1. Introduction

Calcifying microalgae play a major role in global biogeochemical cycling of elements (mainly carbon, calcium and sulphur). Among these species, *Emiliania huxleyi* is well known since it forms very large and dense blooms detectable from space by satellites, due to the highly scattering calcareous plates produced during growth.

Photosynthesis and calcification are biological processes which transform dissolved inorganic carbon (DIC) into respectively particulate organic and inorganic matter which, being denser than seawater, sink towards the ocean floor. The export of particulate organic carbon (POC) from the surface ocean layers, insured by the biological pump, constitutes a carbon sink on a geological scale [8]:

$$6CO_2 + 12H_2O \longrightarrow C_6H_{12}O_6 + 6O_2 + 6H_20 \quad (1)$$

The DIC precipitation into particulate inorganic carbon (PIC), and more specifically into calcium carbonate, also constitutes a sink of carbon, even if calcification produces CO_2 :

$$Ca_2^+ + 2HCO_3^- \longrightarrow CaCO_3 + CO_2 + H_2O \quad (2)$$

Being responsible for almost 70% of the biogenic carbonate precipitation in the oceans, the Coccolithophorid communities have been studied in the context of the predicted increase of CO_2 in the atmosphere resulting from the anthropogenic activity [10]. Based on the accumulation rate of CO_2 observed in the atmosphere from the beginning of the industrial era, current models roughly predict a doubling of the partial pressure of the atmospheric CO_2 (pCO_2) at the end of the 21th century. Since the atmosphere tends to be in equilibrium with the superficial oceanic layers, the change in atmospheric CO_2 will have a direct effect on the CO_2 seawater concentration, and consequently on the carbonate system speciation. For example, [16] have calculated that, if the pCO_2 was doubled in the seawater, the concentration of carbonate should be reduced by 50 % approximately, and the pH by 0.35 units. The consequences are not only on the chemical properties but also on the biological processes. The reductions mentioned above, by diminishing the buffer capacity of sea water, will enhance the production of CO_2 via calcification. Under these conditions, the expected increase of pCO_2 for the next decades would exert a positive feedback on the production of CO_2 by the calcifying communities [9]. Nevertheless, recent studies have shown that cellular calcification could be depressed consequently to a rise of pCO_2 in seawater. For example, by increasing pCO_2 in phytoplankton cultures by the means of strong acid additions, a significant decrease of the calcification rate and of the calcification/photosynthesis ratio was induced in *Gephyrocapsa oceanica* [13, 17], and, with a less extend, in *Emiliania huxleyi*. Therefore, an increase in atmospheric pCO_2 can have antagonistic effects on the production of CO_2 by calcification, so that long term consequences are difficult to predict.

The functional relationships between calcification and photosynthesis continue to cause intense research leading to contradictory results (see [12] for a compilation). The factor influencing calcification are thus still debated, but the only point for which a broad consensus seems to exist is that carbonate CO_3^{2-} is neither used for photosynthesis nor for calcification.

Face to this complex biochemical system, mechanistic models can complement experiments to elucidate the involved processes and to test different simple functional hypotheses, that is not always feasible by the mean of expensive experiments where the variables are not easy to control routinely. We propose here an integrative modelling approach to theoretically explore the interactions between the species of the carbonate system and the processes of photosynthesis and calcification. We consider that the processes of dissolved inorganic carbon uptake, for photosynthesis and calcification are *a priori* driven by a specific carbon species among CO_2 , HCO_3^- or CO_3^{2-} . Moreover, we have considered that these processes could be either coupled or not. To discuss the validity of the different models, we compare the qualitative features predicted by each model to data published in [14]. The experimental device was designed to control in real time the pCO_2 in NO_3-limited chemostat cultures, and allowed to follow accurately the temporal response of net photosynthesis and net calcification of *E. huxleyi* in response to a step elevation of pCO_2 from 360 to 700 ppm. This paper complements the results presented in [2] in the sense that we also examine the quantitative predictions of models that are wrong on a qualitative basis. We show that a reasoning only based on a simple quantitative criterion (least square between data and predictions) would mislead the biological interpretation.

2. Experimental results

The experimental set-up is extensively described in [14, 2]. Two chemostat cultures of the coccolithophore *Emiliania huxleyi* were grown under identical nutrient, temperature, light and pCO_2 conditions. Once the steady state reached in the two cultures, one of them was subjected to an increase in pCO_2 (referred to LH for low to high pCO_2, equivalent to a shift in the sea from 360 μatm to 700 μatm), whereas in the other one the pCO_2 conditions remained unchanged (referred to LL for low to low pCO_2, 360 μatm). It is worth noting that to reproduce this shift in the chemostat, a higher pCO_2 had to be maintained in order to compensate the high biological activity that consumes much more CO_2 than in the sea since biomass is much higher. Indeed, the objective was to double the dissolved CO_2 concentration from a 0.012 mmol.L^{-1} to 0.024 mmol.L^{-1}. This was realised by adjusting pH to the desired value (taking into account the known alkalinity).

During the establishment of the steady state, the two cultures presented identical cell concentrations and diameters, nitrate and nitrite concentrations (near the level of detection), POC and PIC concentrations, pH, pCO_2, total alkalinity (TA), and also similar rates of photosynthesis and calcification. This was a verification that the two cultures were effectively submitted to indistinguishable growth conditions before the pCO_2 shift up made in the LH culture. Table 1 summarises the main differences that appeared between the LL and LH cultures after doubling the pCO_2 in the latter. The most noticeable is a calcification decrease in the LH culture by about 20%, coherent with the decrease of cell diameter, probably due to the loss of external coccoliths. The diminished calcification in the LH culture is also consistent with the observed increase of TA. More surprising is the concomitant decline of the carbon fixation rate, also consistent with the reduction of the cell carbon content. The decrease of the photosynthetic rate being of the same order as that observed for the calcification, the ratio of these two processes remained unchanged.

Quantity	Variation	Unit
POC	-0.023 (-13.5%)	mmolC.L^{-1}
PIC	-0.018 (-11.9%)	mmolC.L^{-1}
DIC	+0.16 (+8.1%)	mmolC.L^{-1}
PON	+0.13 (+0.8 %)	μmolN.L^{-1}
PIC/POC	+0.023 (+2.6 %)	μmolN.L^{-1}
pH	-0.2	
TA	+0.032 (1.3%)	mmol.L^{-1}

Table 1. *Experimental variation of the chemostat quantities after pCO_2 increase, from [14].*

3. Model design

3.1. Introduction

Since the functional dependence between the synthesis of organic and inorganic carbon in *E. huxleyi* are still subject to discussion, as are the related involved regulating mechanisms, we adopted a modelling approach allowing to test different combinations of coupling and regulating variables. These models are kept at a qualitative level to ensure that they are generic and therefore that the derived conclusions are independent of parameter values or even of the shape of the functions used to represent the biological processes. Finally they will be discussed in relation to their ability to qualitatively reproduce the experimental observations previously described.

We have considered 2 classes of models, which suppose respectively that photosynthesis and calcification are either coupled (class CI) or uncoupled (class UI). There is a consensus to admit that HCO_3^- is the substrate of calcification, and that reaction (2) produces CO_2 which can then be used for photosynthesis together with the HCO_3^- and/or CO_2 directly uptaken by the cell. In the proposed series of models we investigated several possibilities for the regulation of these processes, assuming that the regulation is not necessarily driven by the substrate availability, but that it can result from another species concentration, among HCO_3^- , CO_2 and CO_3^{2-} . Therefore, we examined the possibility that, for each class of models (CI or UI) these species can be regulating photosynthesis or calcification. This unusual way of processing will be justified in the sequel, since the simplest model –where HCO_3^- drives calcification and photosynthesis – reveals a contradictory behaviour. Thus, 3 CI and 9 UI models were designed.

The 12 models use the same state variables (Table 2), which makes their comparison possible. The algal biomass in the chemostat (X) is represented by the POC concentration. Particulate nitrogen concentration (N) is taken into account to base a Droop approach [5, 6]. The concentration of nitrate (NO_3) in the chemostat (S_1) is explicitly taken into account since it is the limiting nutrient for growth. Hence the cellular quota of nitrogen (Q) is expressed as the N/X ratio. The dissolved inorganic carbon and calcium (Ca^{2+}) concentrations are denoted D and S_2 respectively. Finally the PIC concentration (C), describes the calcite of both attached and free coccoliths. The concentrations in the chemostat renewal medium are denoted with the subscript "$_{in}$".

The cultures were completely mixed so that the medium in the chemostat was homogeneous. During the experiments pH evolved in the range 7.8 - 8.1. We developed thus

the model making some (classical) simplifying assumptions valid in the realistic pH range 7.6 - 8.3.

First we will present the (classical) equations describing the seawater chemistry since they are a major component of the model to be developed.

3.2. The carbonate system

The ionic balance of the main species in seawater can be written as:

$$[HCO_3^-]+2[CO_3^{2-}]+[B(OH)_4^-]+[OH^-]+[Cl^-]+[Br^-]+[F^-]+2[SO_4^{2-}]+\ldots \quad (3)$$
$$= [Na^+] + [K^+] + 2[Mg^{2+}] + 2[Sr^{2+}] + 2[Ca^{2+}] + [H^+] + \ldots$$

The carbonate alkalinity (CA) represents the electric charges carried in the carbonate system:

$$CA = [HCO_3^-] + 2[CO_3^{2-}] \quad (4)$$

The total alkalinity (TA) is defined by:

$$TA = CA + [B(OH)_4^-] + [OH^-] - [H^+] \quad (5)$$

Note that this definition indeed corresponds to the practical alkalinity which is a very good approximation of the total alkalinity [16].

We denote $\lambda = TA - 2[Ca^{2+}] = TA - 2S_2$.

In a first approximation, the ions mainly contributing to λ depend on the salinity and remain constant.

In a first step, to keep the model mathematically tractable, we will also assume that $\lambda_0 = [B(OH)_4^-] + [OH^-] - [H^+]$ remains constant compared to CA. This hypothesis implies mainly that $[B(OH)_4^-]$ hardly varies, which is reasonable for the considered pH range since, its associated dissociation constant is $pK_B = 8.6$. However, the detailed computation when explicitly taking into account variations of borate is presented in Appendix B.

From the previous considerations carbonate alkalinity is thus only depending on calcium: $CA = \lambda - \lambda_0 + 2S_2$. In order to compute the $[HCO_3^-]$ and $[CO_3^{2-}]$ concentrations, we will use the dissociation constants of the carbon dioxide (K_1) and bicarbonate (K_2) (the proton concentration, $[H^+]$ will be denoted h):

$$K_1 = \frac{h[HCO_3^-]}{[CO_2]} \text{ and } K_2 = \frac{h[CO_3^{2-}]}{[HCO_3^-]} \quad (6)$$

The total dissolved inorganic carbon (D) is defined as:

$$D = [HCO_3^-] + [CO_3^{2-}] + [CO_2] \quad (7)$$

Note that, in the considered pH range, we have $[HCO_3^-] >> [CO_3^{2-}] >> [CO_2]$ (see for example [16]). It follows that bicarbonate is the main carbon species in the bicarbonate system:

$$[HCO_3^-] \simeq D \quad (8)$$

We deduced from equations (4) and (7), in the considered pH range:

$$[CO_3^{2-}] \simeq CA - D \tag{9}$$

Although this approximation will be useful for the mathematical analysis, we will compute the exact relationship between the carbonic species and pH.

Let us now compute the following ratio: $r = \frac{D}{CA}$, using equations (4), (7) and (6), we get:

$$r = \frac{h + K_2 + h^2/K_1}{h + 2K_2} \tag{10}$$

It follows that h can be computed as a function of r:

$$h = u(r) = \left(-1 + r + \sqrt{(1-2r)(1-4K_2/K_1) + r^2}\right)\frac{K_1}{2} \tag{11}$$

where it can be verified that function u is an increasing function of r. Note that pH is directly deduced from (11). Now using equations (6) and (4) we can compute the exact CO_2 concentration:

$$[CO_2] = \frac{CA}{K_1}\frac{h^2}{h + 2K_2} = CA\, v(r) = \psi(S_2, D) \tag{12}$$

where $v(r) = \frac{1}{K_1}\frac{u(r)^2}{u(r)+2K_2}$ is an increasing function of u and thus an increasing function of r. As shown on Figure 1, CO_2 is an increasing function of D and a decreasing function of S_2 and pH is increasing with respect to S_2 and decreasing with respect to D.

Finally the coccoliths dissolution rate should be taken into account. However, the dissolution of coccoliths (mainly composed of calcite) is possible if the $CaCO_3$ saturation state Ω of the medium is lower than one:

$$\Omega = \frac{[Ca^{2+}][CO_3^{2-}]}{K_{sp}} \tag{13}$$

where the solubility constant yields $K_{sp} = 5.1510^{-7} mol^2.L^{-2}$. The computation of the saturation state shows that Ω is always above 2.5 during the experiment. Hence conditions for calcite solubilisation are not met and this phenomenon is not taken into account in the model.

4. The coupled models (CI)

4.1. General formulation

In the CI class models, photosynthesis and calcification are coupled so that the carbon assimilation for the coccoliths (C) and for the biomass (X) can be represented as follows:

$$\frac{1-\alpha}{\alpha}S_2 + \frac{1}{\alpha}D \quad \stackrel{\mu(.)X}{\longrightarrow} \quad \frac{1-\alpha}{\alpha}C + X \tag{14}$$

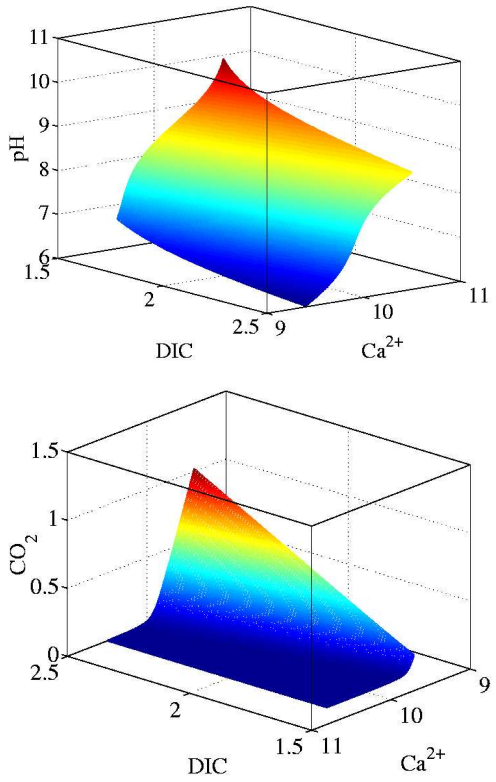

Figure 1. *CO_2 and pH as functions of D and Ca^{2+}.*

where $\mu(.)$ represents the specific algal growth rate. The coupling between photosynthesis and calcification induces the same expression $\mu(.)X$ for the kinetics of these two processes. The constant α represents the proportion of the total up taken DIC which is allocated to photosynthesis.

Following the quota model viewpoint [5, 4, 6], we consider that growth and external NO_3 uptake are uncoupled. The nitrogen mass transfer is thus given by:

$$S_1 \xrightarrow{\rho(.)X} N \tag{15}$$

	Meaning	Unit
D	Dissolved inorganic carbon (DIC)	$mmol.L^{-1}$
N	Particulate nitrogen (PON)	$mmol.L^{-1}$
Q	Internal nitrogen quota	/
X	Particulate organic carbon (POC)	$mmol.L^{-1}$
C	Coccoliths concentration (PIC)	$mmol.L^{-1}$
S_1	Nitrate	$mmol.L^{-1}$
S_2	Calcium	$mmol.L^{-1}$

Table 2. *Meaning of the state variables whose evolution is described by each of the 12 proposed models.*

where N is the algal nitrogen and $\rho(.)$ the external NO_3 uptake rate.

The carbon exchanges between the liquid and gaseous phases are described by Henry's law:

$$qC = K_L a(CO_2 - K_H pCO_2)$$

where $K_L a$ is the gas transfer rate, K_H is Henry's constant and pCO_2 represents the partial pressure of carbon dioxide in the gaseous phase.

We can now straightforwardly [1, 3] derive from the mass transfer equations (14) and (15) the mass balance based model:

$$\dot{S}_1 = d(S_{1in} - S_1) - \rho(.)X \quad (16)$$

$$\dot{D} = d(D_{in} - D) - \frac{1}{\alpha}\mu(.)X - qC \quad (17)$$

$$\dot{Q} = \rho(.) - \mu(.)Q \quad (18)$$

$$\dot{X} = -dX + \mu(.)X \quad (19)$$

$$\dot{C} = -dC + \frac{1-\alpha}{\alpha}\mu(.)X \quad (20)$$

$$\dot{S}_2 = d(S_{2in} - S_2) - \frac{1-\alpha}{\alpha}\mu(.)X \quad (21)$$

Note that the equation for Q is obtained from Equation (17) combined with the equation of N:

$$\dot{N} = -dN + \rho(.)X$$

It is worth noting that this representation is valid whatever the real substrate used for photosynthesis and calcification and whatever the dissolved inorganic component driving photosynthesis and calcification. Now we need to provide an analytical expression for the growth and uptake rates.

4.2. Kinetic modelling

To remain as general as possible in the formalisation of $\rho(.)$ and $\mu(.)$, very simple hypotheses are adopted. We assume that $\rho(.)$ is an increasing function of the NO_3 concentration (S_1), and that $\mu(.)$ is an increasing function of both the internal nitrogen quota (Q) and the DIC species (Dp) selected for its role in the regulation of growth and calcification. It must be emphasised, at this level, that the qualitative analysis presented later on to determine the qualitative response to a pCO_2 increase, remains valid for any functions $\rho(S_1)$ and $\mu(Q, Dp)$ with the considered properties.

Nevertheless, in order to compute the range of variations and to compare simulations with data, we will use the Michaelis-Menten expression to represent the NO_3 uptake rate [7], $\rho(S_1) = \rho_m S_1/(S_1 + k_N)$, where ρ_m and k_N are the maximum uptake rate and the half-saturation constant, respectively. Based on the Droop model [5, 6], the net growth rate may be written as:

$$\mu(Q, Dp) = \bar{\mu}(1 - \frac{k_Q}{Q})\frac{Dp}{Dp + k_D p} - R \quad (22)$$

where k_Q, $\bar{\mu}$ and k_{Dp} are respectively the subsistence internal quota, the maximum hypothetical growth rate and the half-saturation constant for the chosen regulating carbon species, and R the respiration rate (supposed to be constant).

4.3. Model equations

The following differential system synthesises the previous developments for a regulating species Dp.

$$\dot{S}_1 = d(S_{1in} - S_1) - \rho(S_1)X \quad (23)$$

$$\dot{Q} = \rho(S_1) - \mu(Q, Dp)Q \quad (24)$$

$$\dot{X} = -dX + \mu(Q, Dp)X \quad (25)$$

$$\dot{C} = -dC + \frac{1-\alpha}{\alpha}\mu(Q, Dp)X \quad (26)$$

$$\dot{D} = d(D_{in} - D) - \frac{1}{\alpha}\mu(Q, Dp)X - K_L a(\psi(S_2, D) - K_H pCO_2) \quad (27)$$

$$\dot{S}_2 = d(S_{2in} - S_2) - \frac{1-\alpha}{\alpha}\mu(Q, Dp)X \quad (28)$$

The 3 models of the CI class, named CI-HCO_3^- , CI-CO_2 , CI-CO_3^{2-} differ only by the inorganic carbon component Dp controlling photosynthesis and calcification.

Remark: for very high value of the transfer coefficient $K_L a$, compared to the terms related to chemostat hydraulics ($d(D_{in} - D)$) and to biological activity ($\frac{1}{\alpha}\mu(Q, Dp)X$), Equation (27) shows that D will rapidly reach its pseudo steady-state corresponding to $CO_2^* = K_H pCO_2$. The carbonate system is then mainly constrained by the applied pCO_2. The high bubbling flow rate in the chemostat experiments guaranty a high $K_L a$: in the sequel we will apply this classical hypothesis for the mathematical analysis of the model.

4.4. Carbon assimilation rate

The carbon assimilation rate by photosynthesis [resp. by calcification] will be named Φ_p [resp. Φ_c] and called rate of photosynthesis [resp. of calcification] for short. For the CI class models, the coupled uptake and use of DIC for photosynthesis and calcification is expressed by the following equation:

$$\Phi_c = \frac{1-\alpha}{\alpha}\mu(Q, Dp)X, \quad \Phi_p = \mu(Q, Dp)X \quad (29)$$

The total carbon assimilation rate is denoted $\Phi = \Phi_c + \Phi_p = \frac{1}{\alpha}\mu(Q, Dp)X$.

The total specific carbon assimilation rate (Φ), is thus:

$$\Phi = \frac{1}{\alpha}\mu(Q, Dp) \quad (30)$$

5. The uncoupled models

5.1. General formulation

This class of models supposes that calcification and photosynthesis are uncoupled, so that incorporation of inorganic carbon follows two different metabolic pathways:

$$\begin{array}{rcl} D & \stackrel{\mu(.)X}{\longrightarrow} & X \\ S_2 + D & \stackrel{\sigma(.)X}{\longrightarrow} & C \end{array} \tag{31}$$

where $\mu(.)$ and $\sigma(.)$ are the rate of photosynthesis and calcification, respectively. The process of nitrogen uptake is still assumed to be independent from carbon assimilation and follows thus reaction (15).

5.2. Kinetic description

The rate of photosynthesis, $\mu(Q, Dp)$, is an increasing function of both the internal nitrogen quota and the regulating species Dp . Calcification is assumed to be an increasing function $\sigma(.)$ of the calcification regulating species Dc .

As it will be discussed in the sequel, the qualitative response to a pCO_2 increase is, as for the CI class models, independent of the mathematical form chosen for $\sigma(Dc)$ and $\mu(Q, Dp)$, and of the parameter values (except in particular cases, mentioned below).

In order to quantify the variation range, we will consider that photosynthesis is expressed, as in the CI class models, by expression (22), and that the calcification rate is an increasing function of the variable Dc :

$$\sigma(Dc) = \sigma_m \frac{Dc}{Dc + k_{Dc}}$$

5.3. Model equations

The following equations give the structure adopted for the UI class models :

$$\dot{S}_1 = d(S_{1in} - S_1) - \rho(S_1)X \tag{32}$$

$$\dot{Q} = \rho(S_1) - \mu(Q, Dp)Q \tag{33}$$

$$\dot{X} = -dX + \mu(Q, Dp)X \tag{34}$$

$$\dot{C} = -dC + \sigma(Dc)X \tag{35}$$

$$\dot{D} = d(D_{in} - D) - \mu(Q, Dp)X - \sigma(Dc)X - K_L a(\psi(S_2, D) - K_H pCO_2) \tag{36}$$

$$\dot{S}_2 = d(S_{2in} - S_2) - \sigma(Dc)X \tag{37}$$

There are 9 possible combinations for Dp and Dc for this equation system, depending on the regulating carbon species for calcification and photosynthesis among CO_2 , HCO_3^- and CO_3^{2-} . For example, in the model denoted UI-HCO_3^--CO_2. $Dp = HCO_3^-$ and $Dc = CO_2$

Remark: as for the CI models, for very high values of the transfer coefficient K_La, the terms related to chemostat hydraulics and to biological activity can be neglected in Equation (36) therefore leading to $CO_2^* = K_H pCO_2$. The carbonate system is then mainly constrained by the applied pCO_2.

5.4. carbon assimilation

In this model, total carbon assimilation is different for photosynthesis and calcification:

$$\Phi_p = \mu(Q, Dp)X \text{ and } \Phi_c = \sigma(Dc)X \tag{38}$$

And the total rate of carbon assimilation per biomass unit is thus:

$$\Phi = \mu(Q, Dp) + \sigma(Dc) \tag{39}$$

6. Study of the qualitative response of the set of models

6.1. Introduction

In order to determine which regulation mechanism is the most appropriate, we will assess the qualitative model consistency with respect to experimental observations. Hence we will study the qualitative behaviour for both classes of models (coupled or uncoupled) and for all the considered potential regulating species. This analysis is to be performed in the framework of general (increasing) functions $\mu(.)$, $\rho(.)$ and $\sigma(.)$, and it is therefore independent of the parameter values (except in particular cases that will be mentioned) and will provide a diagnosis on the model adequacy. This analysis will be performed at steady-state. It will mainly consist in determining the evolution of the equilibrium of the model when the CO_2 partial pressure is increased. In other terms, if x_i^* is a state variable of a given model at equilibrium (steady-state will be marked with *), we will investigate the sign of $\frac{\partial x_i^*}{\partial pCO_2}$.

At steady-state, the state variables of any model in the considered set verify:

$$\dot{S}_1 = \dot{D} = \dot{X} = \dot{C} = \dot{Q} = \dot{S}_2 = 0 \tag{40}$$

In the sequel, we will use these equations to determine the effect of an increase in pCO_2 on the system. We will first derive some general properties that are valid for any of the 12 considered models. Then we will separately consider the CI and the UI models.

6.2. Qualitative properties of S_1, X and Q for the UI and CI models

It is worth noting that the equations for S_1, X and Q are the same for the two sets of models. This remark leads to the following property:

Property 1 *For any UI or CI model where photosynthesis is controlled by Dp, we have:*

$$\bullet \frac{\partial Q^*}{\partial Dp^*} < 0 \tag{41}$$

$$\bullet \frac{\partial X^*}{\partial Dp^*} > 0 \tag{42}$$

$$\bullet \frac{\partial S_1^*}{\partial Dp^*} < 0 \tag{43}$$

Proof: With the biomass equations (25) or (34) we get :

$$\mu(Q^*, Dp^*) = d \tag{44}$$

By differentiating this equation with respect to Dp, we obtain:

$$\frac{\partial \mu}{\partial Q^*}\frac{\partial Q^*}{\partial Dp^*} + \frac{\partial \mu}{\partial Dp^*} = 0 \tag{45}$$

Since μ is an increasing function of both Q and Dp, we end up with Equation (41).

Combining equations (32) to (34), we have:

$$S_1^* + Q^* X^* = S_{1in} \tag{46}$$

Since in standard chemostat experiments NO_3 is limiting, we have $S_1^\star << S_{1in}$, it follows that $X^* \simeq \frac{S_{1in}}{Q^*}$, leading thus to (42).

Finally from equation (23) or (32), we get

$$\frac{\partial S_1^*}{\partial Dp^*}(\frac{d\rho}{dS_1}X^* + d) = -\rho(S_1)\frac{\partial X^*}{\partial Dp^*} < 0 \tag{47}$$

and then we obtain (43). ■

6.3. Qualitative properties of the CI models for C, S_2 and D

Property 2 *For any CI model where photosynthesis and calcification are controlled by Dp, we have:*

$$\bullet \frac{\partial C^*}{\partial Dp^*} > 0 \tag{48}$$

$$\bullet \frac{\partial (C^*/X^*)}{\partial Dp^*} = 0 \tag{49}$$

$$\bullet \frac{\partial S_2^*}{\partial Dp^*} < 0 \tag{50}$$

Finally, for Dp $\neq CO_3^{2-}$ *, we have* $\frac{\partial D^*}{\partial Dp^*} > 0$ *and* $\frac{\partial CO_2*}{\partial Dp^*} > 0$. *For Dp =*$CO_3^{2-}$ *, we have* $\frac{\partial D^*}{\partial Dp^*} < 0$ *and* $\frac{\partial CO_2*}{\partial Dp^*} < 0$.

Moreover, in all the cases $\frac{\partial D^*}{\partial CO_2*} > 0$.

Proof: Note first, that from equations (25) and (26), biomass and coccoliths are correlated:

$$C^* = \frac{1-\alpha}{\alpha}X^* \tag{51}$$

Moreover, from equation (28), we have

$$S_{2in} - S_2^* = \frac{1-\alpha}{\alpha} X^* \tag{52}$$

These two equations combined with (42) lead to (49) and (50).

Now let us compute now the sign of $\frac{\partial CO_2*}{\partial Dp^*}$ and $\frac{\partial CO_2*}{\partial D^*}$. Note first that when the biological activity is negligible, the standard and well-known properties of sea water [16] straightforwardly lead to: $\frac{\partial CO_2}{\partial HCO_3^-} > 0$, $\frac{\partial CO_2}{\partial CO_3^{2-}} < 0$ and $\frac{\partial CO_2}{\partial D} > 0$. However due to biological activity these relationships are not straightforward anymore for high biomass concentrations.

The computation of $\frac{\partial CO_2*}{\partial Dp^*}$ is trivial for Dp $=CO_2$. For Dp $=HCO_3^-$, figure 2 illustrates the fact that CO_2 , computed from equation (12) is an increasing function of HCO_3^- and a decreasing function of S_2: $CO_2 = \psi_{CO_2-HCO_3^-}(HCO_3^-, S_2)$.

Note that this is valid for the simplified computation or for the one integrating borate effects developed in Appendix A. As a consequence

$$\frac{\partial CO_2*}{\partial Dp^*} = \frac{\partial \psi_{CO_2-HCO_3^-}}{\partial Dp^*} + \frac{\partial \psi_{CO_2-HCO_3^-}}{\partial S_2^*} \frac{\partial S_2^*}{\partial Dp^*}$$

is positive since $\frac{\partial S_2^*}{\partial Dp^*} < 0$.

Now for Dp $=CO_3^{2-}$, it can be checked (Figure 2) that, in the considered pH range, CO_2 is a decreasing function of CO_3^{2-} and an increasing function of S_2: $CO_2 = \psi_{CO_2-CO_3^{2-}}(CO_3^{2-}, S_2)$.

As a consequence, $\frac{\partial \psi_{CO_2-CO_3^{2-}}}{\partial CO_3^{2-*}} + \frac{\partial \psi_{CO_2-CO_3^{2-}}}{\partial S_2*} \frac{\partial S_2^*}{\partial CO_3^{2-*}} < 0$.

Now let us examine the sign of $\frac{\partial D*}{\partial Dp^*}$. When $D_p = CO_3^{2-}$ we consider the increasing function ψ_{D-CO_2} such that $D = \psi_{D-CO_2}(CO_2, S_2)$. We have then

$$\frac{\partial D^*}{\partial CO_2^*} = \frac{\partial \psi_{D-CO_2}}{\partial CO_2} + \frac{\partial \psi_{D-CO_2}}{\partial S_2} \frac{\partial S_2}{\partial D_p^*} \frac{\partial D_p^*}{\partial CO_2^*}$$

Since $\frac{\partial S_2}{\partial D_p^*} < 0$ and $\frac{\partial D_p^*}{\partial CO_2^*} < 0$ it shows that $\frac{\partial D^*}{\partial CO_2^*} > 0$.

When $D_p = CO_2$ we consider function $D = \psi_4(CO_2, S_2)$. We have thus:

$$\frac{\partial D^*}{\partial CO_2^*} = \frac{\partial \psi_4}{\partial CO_2} + \frac{\partial \psi_4}{\partial S_2} \frac{\partial S_2}{\partial CO_2^*}$$

In this case, a numerical evaluation is necessary. $\frac{\partial D^*}{\partial CO_2^*}$ has been computed using the analytical expression of $\frac{\partial S_2}{\partial CO_2^*}$ and the numerical values of $\frac{\partial \psi_4}{\partial CO_2}$ and $\frac{\partial \psi_4}{\partial S_2}$. These calculations have been done 200 times for different combinations of parameter values, considering possible variations of $\pm 10\%$ of the parameter nominal values (as presented in Tables 5 and 6). The range of variations for a $\pm$10% variation of the parameters leads to $\frac{\partial D^*}{\partial CO_2^*} \in [7.7\ 17.1]$ which is thus positive.

The same method is applied when $D_p = HCO_3^-$ using $D = \psi_{D-HCO_3^-}(HCO_3^-, S_2)$, and shows that $\frac{\partial D^*}{\partial HCO_3^{-*}} \in [0.61\ 1.57]$ which is thus positive ■

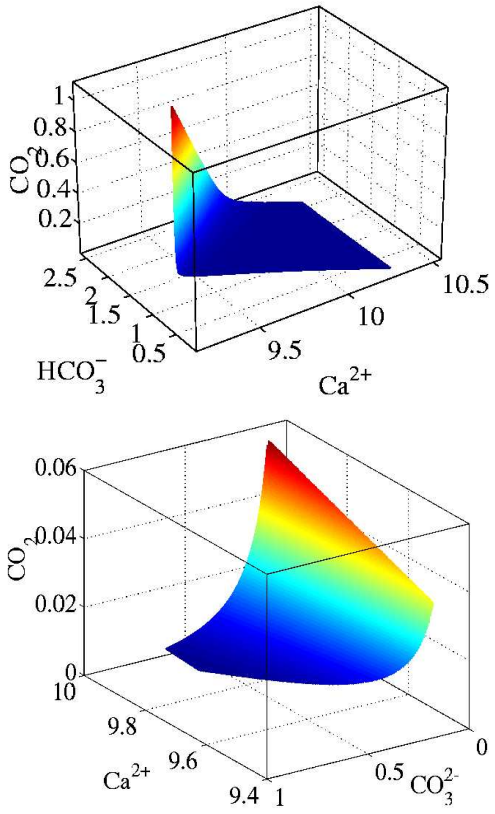

Figure 2. *Evolution of functions* $\psi_{CO_2-CO_3^{2-}}(CO_3^{2-}, S_2)$ *and* $\psi_{CO_2-HCO_3^-}(HCO_3^-, S_2)$.

6.4. Response of the carbon assimilation rate for the CI models

Property 3 *The photosynthesis* (Φ_p) *and calcification* (Φ_c) *rates are increasing functions of* pCO_2 *for models CI-*HCO_3^- *and CI-*CO_2*. They are decreasing for CI-*CO_3^{2-}*. The total carbon incorporation rate per biomass unit remains constant despite the change in* pCO_2.

Proof: The total carbon incorporation at equilibrium can be computed for all the CI models from (30):

$$\Phi^* = \frac{1}{\alpha} dX^* = \frac{1}{\alpha}\Phi_p^* = \frac{1}{1-\alpha}\Phi_c^* \tag{53}$$

Therefore, the evolutions of Φ^*, Φ_p^* and Φ_c^* follow the evolution of X^*.

■

6.5. Study of the qualitative properties of the UI models for C, S_2 and D

Property 4 *For any UI model where photosynthesis and calcification are controlled respectively by Dp and Dc, we have:*

$$\bullet \frac{\partial C^*}{\partial Dc^*} = -\frac{\partial S_2^*}{\partial Dc^*} \tag{54}$$

$$\bullet \frac{\partial (C^*/X^*)}{\partial Dc^*} > 0 \tag{55}$$

• *For models UI-HCO_3^- -CO_3^{2-} , UI-CO_2 -CO_3^{2-} UI-CO_3^{2-} -HCO_3^- and UI-CO_3^{2-} -CO_3^{2-} we have $\frac{\partial S_2^*}{\partial CO_2^*} > 0$ otherwise $\frac{\partial S_2^*}{\partial CO_2^*} < 0$. Finally, in all the cases $\frac{\partial D^*}{\partial CO_2^*} > 0$.*

Note that the last point of this property is straightforward for low biomass concentrations [16].

Proof: Let us first remark that from (37) and (35) we get

$$C^* + S_2^* = S_{2in}^*$$

this provides equation (54). From equation (35), it follows:

$$C = \frac{X}{d}\sigma(Dc) \tag{56}$$

This leads to (55).

To demonstrate the last point we use equation (44). At steady state $S_1^\star << S_{1in}$, we can thus rewrite this equation as:

$$\mu_a(\frac{S_{1in}}{X^*})\mu_b(Dp^*) = d \tag{57}$$

This equation can be used to derive the expression of X^* from Dp^*: $X^* = \omega(Dp^*)$, where $\omega(Dp^*)$ is obviously an increasing function.

Note that for the numerical computations, the function ω associated to the Droop model can be computed as follows:

$$\omega(Dp) = \frac{S_{1in}}{k_Q}[1 - \frac{d+R}{\bar{\mu}}(1 + \frac{k_{Dp}}{Dp})] \tag{58}$$

S_2 can be related to Dp^* and Dc^* using $S_{2in}^* - S_2^* = \frac{X^*}{d}\sigma(Dc^*)$ it yields:

$$S_2^* = S_{2in}^* - \frac{1}{d}\omega(Dp^*)\sigma(Dc^*) \tag{59}$$

The proof of the last statement of Property 4, is detailed in Appendix B, considering successively 2 main cases. The proof is based on a semi-quantitative study of the signs of $\frac{\partial S_2^*}{\partial Dp^*}$ and $\frac{\partial Dc^*}{\partial Dp^*}$ (see Table 3).

■

Model	A_1	A_2	B_1	B_2	$\frac{\partial S_2}{\partial Dp^*}$	$\frac{\partial Dc^*}{\partial Dp^*}$	$\frac{\partial S_2}{\partial CO_2^*}$
UI-CO_2 -CO_3^{2-}	+	-	[-38.2 -2.72]	+	+	-	+
UI-HCO_3^- -CO_3^{2-}	+	-	[-13.0 -5.3]	+	+	-	+
UI-CO_3^{2-} -CO_2	+	-	[-4.6 -1.35]	+	+	-	-
UI-CO_3^{2-} -HCO_3^-	+	-	[-0.22 -0.092]	+	-	-	+
UI-CO_2 -HCO_3^-	+	+	+	[-0.38 -0.042]	-	+	-
UI-HCO_3^- -CO_2	[-4.2 -1.81].10^{-3}	+	+	+	-	+	-

Table 3. *Qualitative or semi-quantitative study of the signs of $\frac{\partial Dc^*}{\partial Dp^*}$ and $\frac{\partial S_2}{\partial CO_2^*}$*

6.6. Response of the carbon incorporation rate for the UI models

Property 5 *The total carbon incorporation rate (Φ), the photosynthesis (Φ_p) and calcification (Φ_c) rates are increasing functions of pCO_2 for all the models where CO_3^{2-} does not intervene as a regulating species. For models where CO_3^{2-} is a regulating species, Φ decreases. These results are generic except for models UI-HCO_3^--CO_3^{2-}, UI-CO_2-CO_3^{2-} and UI-CO_3^{2-}-CO_2 where parameter values have been used for the Φ predictions.*

The specific photosynthesis rate is constant whereas the calcification rate decreases for Dc =CO_3^{2-} and increases in the other cases.

Proof: The carbon incorporation rates at equilibrium can be computed from (38):

$$\Phi_p^* = dX^*, \quad \Phi_c^* = dC^* \tag{60}$$

They have the same trend as X^* and C^* respectively.

For the total incorporation rate $\Phi^* = d(X^* + C^*)$, we can directly conclude when X^* and C^* have the same trend, *i.e.* when $\frac{\partial Dp^*}{\partial Dc^*} > 0$. For the three cases UI-HCO_3^--CO_3^{2-}, UI-CO_2-CO_3^{2-} and UI-CO_3^{2-}-CO_2 this result was obtained from a numerical computation.

Remark: The photosynthesis to calcification ratio $\frac{\Phi_p^*}{\Phi_c^*}$ has the same response to pCO_2 as $\frac{X^*}{C^*}$.

6.7. Synthesis

It is now possible to summarise the qualitative behaviour for each state variable in response to increased pCO_2. Table 4 presents this evolution for the 12 considered models, depending on the carbon compounds driving the process. We lay emphasise on the fact that these results have been deduced mainly from qualitative arguments that do not depend on parameter values, and as such they are very insensitive to modelling options. Parameter ranges were considered to deal with high biomass concentrations where intuition for the prediction of the carbonate system could be contradicted. However it is shown that in the considered experimental conditions the "classical" evolution of the carbonate system is still valid (*i.e.* $\frac{\partial CO_2}{\partial HCO_3^-} > 0$, $\frac{\partial CO_2}{\partial CO_3^{2-}} < 0$ and $\frac{\partial CO_2}{\partial D} > 0$).

The first outcome of this qualitative study is that the models where HCO_3^- would straightforwardly drive photosynthesis and calcification (model CI-HCO_3^- or UI-HCO_3^- -HCO_3^-) predict increase of POC and PIC as well as calcification and photosynthesis

	CI			UI							
	HCO_3^-	CO_2	CO_3^{2-}	HCO_3^- HCO_3^-	HCO_3^- CO_2	HCO_3^- CO_3^{2-}	CO_2 HCO_3^-	CO_2 CO_2	CO_2 CO_3^{2-}	CO_3^{2-} HCO_3^-	CO_3^{2-} CO_2	CO_3^{2-} CO_3^{2-}
D *	↗	↗*	↗	↗	↗*	↗*	↗*	↗	↗*	↗*	↗*	↗
Dp *	↗	↗	↘	↗	↗*	↗*	↗	↗	↗*	↘*	↘*	↘
Dc *	↗	↗	↘	↗	↗	↘*	↗*	↗	↘*	↗*	↗	↘
X*	↗	↗	↘	↗	↗	↗	↗	↗	↗	↘	↘	↘
Q*	↘	↘	↗	↘	↘	↘	↘	↘	↘	↗	↗	↗
S_1^*	↘	↘	↗	↘	↘	↘	↘	↘	↘	↗	↗	↗
C *	↗	↗	↘	↗	↗	↘	↗	↗	↘	↘	↗	↘
S_2^*	↘	↘	↗	↘	↘*	↗*	↘*	↘	↗*	↗*	↘*	↗
$\frac{C^*}{X^*}$	→	→	→	↗	↗	↘	↗	↗	↘	↗	↗	↘
pH*	↘	↘	↘	↘	↘	↘	↘	↘	↘	↘	↘	↘
CA	↘	↘	↗	↘	↘	↗	↘	↘	↗	↗	↘	↗
TA	↘	↘	↗	↘	↘	↗	↘	↘	↗	↗	↘	↗
Φ^*	↗	↗	↘	↗	↗	↘*	↗	↗	↘*	↘	↘*	↘
Φ_p^*	↗	↗	↘	↗	↗	↗	↗	↗	↗	↘	↘	↘
Φ_c^*	↗	↗	↘	↗	↗	↘	↗	↗	↘	↘	↗	↘
$\frac{\Phi_p^*}{\Phi_c^*}$	→	→	→	↘	↘	↗	↘	↘	↗	↘	↘	↗

Table 4. *Qualitative variations of the state variables at steady-state after an elevation of pCO_2 for the 12 considered models. Symbol * means that interval based numerical estimations were performed to conclude.*

rates; this is contradicted by the experiment. In the same way, model UI-CO_2 -HCO_3^- predicts a contradictory response. Indeed, all the models where only species CO_2 and/or HCO_3^- are involved have predictions that are contrary to experimental evidence. It is noteworthy that these 6 models have exactly the same qualitative behaviour. The only difference between the two groups is their C/X predictions (constant for the CI models and increasing for the UI models), and their photosynthesis over calcification ratio (constant for the CI models and decreasing for the UI models). It therefore follows that CO_3^{2-} is required in the model to explain the experimental observations.

Among the considered models, only the models where CO_3^{2-} regulates photosynthesis are compatible with the experimental decrease of POC and PIC. The 3 remaining models only differ by their predictions of the PIC over POC ratio and photosynthesis over calcification ratio: C/X and Φ_c^*/Φ_p^* increase for model UI-CO_3^{2-} -HCO_3^- , they are constant for model CI-CO_3^{2-} while they decrease for UI-CO_3^{2-} -CO_3^{2-} . The slight observed experimental increase of the PIC over POC ratio (see Table 1) is not significant and cannot be used to select one of these 3 models. Note however that if another experiment could validate a significant increase of this ratio, the most appropriate model would be UI-CO_3^{2-} -HCO_3^- , where photosynthesis is regulated by CO_3^{2-} and calcification by HCO_3^- .

It is important to note that the considered experimental results differ from those of [13, 17] which were obtained in unlimited growth conditions (a decrease of C/X was observed).

7. Quantitative approach trough numerical simulations

Note first that from the previous qualitative analysis it is possible to discuss which model can explain the observed response with respect to pCO_2 increase. However, here we discuss the ability of all the models to quantitatively lie in a reasonable range of the data.

We first briefly describe how the parameter values have been obtained. The objective was to find a parameter set that minimise a least square error criterion *i.e.* such that

numerical simulation are close to the experimental data. Parameter K_H has been taken from the literature [16]. Parameters $\bar{\mu}$, k_Q, ρ_m and k_N were estimated from batch experiments where nitrate uptake and biomass were simultaneously measured. Parameter α was computed from the fraction of biomass and coccoliths at steady state (see Equation (51)), and parameter σ_m was derived from Equation (56). The respiration rate has been neglected ($R = 0$). Finally, parameters k_{Dp}, k_{Dc} and K_La were obtained using a least square approach, where distance between simulations and measured data were minimised using the Matlab *fmins* function.

Finally, the parameter values and units are presented in Table 5 for the 12 considered models.

Parameters	Values	Units
d	0 to 0.5	d^{-1}
S_{1in}	12.5	$\mu molN.L^{-1}$
D_{in}	2.29	$mmolC.L^{-1}$
K_La	1.75	d^{-1}
ρ_m	100.19	$\mu molN.mmolC^{-1}.d^{-1}$
k_{S_1}	0.038	$\mu molN.L^{-1}$
K_1	$1.392\,10^{-6}$	$mmol.L^{-1}$
K_2	$1.189\,10^{-9}$	$mmol.L^{-1}$
K_H	36.7	$mmolCO_2.L^{-1}.\mu$atm
λ	-17.31[3]	mmol.L^{-1}
λ_0	0.086[3]	mmol.L^{-1}

Table 5. *Estimates of the model parameters for model UI-CO_3^{2-} -HCO_3^- .*

Parameters	HCO_3^-	CO_3^{2-}	CO_2	pH	Units
k_{Dp}	1.65	0.16	0.015	$1.5\,10^{-8}$	$\mu molC.L^{-1}$
k_{Dc}	1.65	0.12	0.015	$1.5\,10^{-8}$	$\mu molC.L^{-1}$
k_Q	34.4	28.2	61.03	34.4	$\mu molN.mmolC^{-1}$
$\bar{\mu}$	2.22	1.61	5.62	1.78	d^{-1}
σ_m	0.83	0.83	0.8	0.8	d^{-1}

Table 6. *Parameters used to fit the model to the data.*

The computations were performed over 42 simulated days. The first 18 days were necessary to ensure that a steady-state had been reached for each variable. The partial pressure of carbon dioxide (pCO_2) was then instantly doubled (360 μatm to 700 μatm), with increase of bubbling (corresponding to a strong increase in K_La) during 30 minutes. and the numerical behaviour of the system was observed for a further 16 days. In Figures 3, 4 and 5 model simulations are compared to experimental data.

The model-computed evolution of nitrate fits the data very well for any of the considered models. In each case the predicted model values and the experimental data (Figure 3) show a rapid decrease in nitrate concentrations over the first 3 days. For the remaining simulation period, the nitrate concentrations stay at a very low level (below the detection threshold). No change is detectable after the doubling of pCO_2.

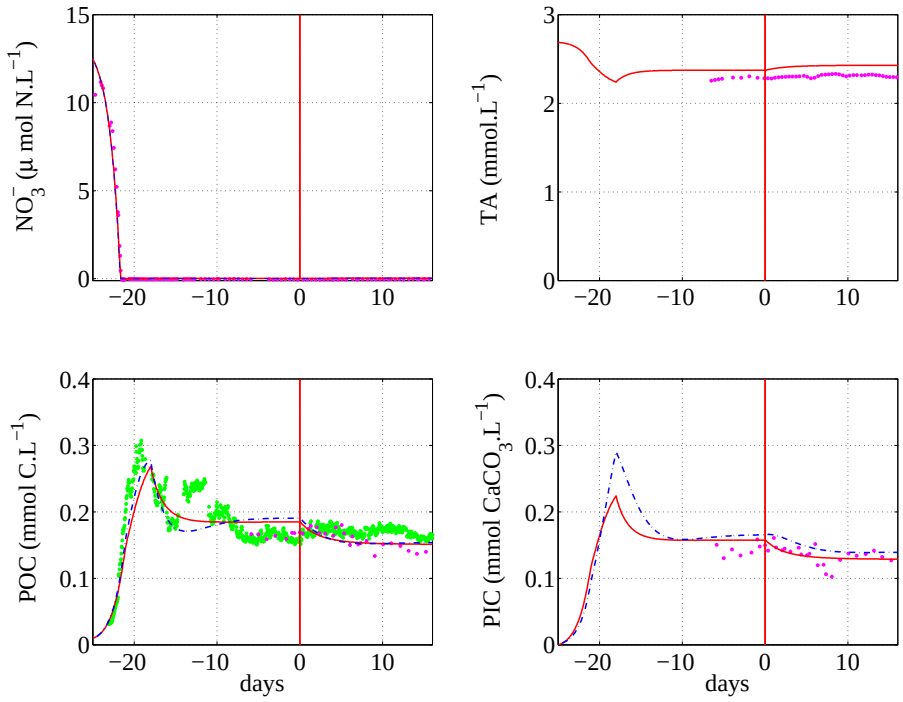

Figure 3. *Comparison between models CI-CO_3^{2-} (—), UI-CO_3^{2-} -HCO_3^- (- · -) and data for POC (X), PIC (C) Nitrate (S_1) and TA. Organic carbon is simultaneously estimated by biovolume (light grey points).*

The evolution of the carbonate system (Figure 4) is accurately predicted by the models for all the considered models. The increase in the simulated DIC in response to the pCO_2 elevation is well reproduced. Note that the carbonate system and the pH are also well reproduced by models which are *a priori*, as previously demonstrated, not adapted (see Figure 7).

As expected, in the simulations where the photosynthesis controlling species are HCO_3^- or CO_2, we observe an increase in biomass in response to the shift in pCO_2 (Figure 6). In contrast when CO_3^{2-} is the limiting species we notice a depletion of the biomass. This evolution of the biomass and calcium carbonate (Figure 3) is quantitatively consistent with the data. This could justify to test only the four corresponding models. However, in the spirit of a more general reflection on model validation and result presentation, we have also calibrated the models whose qualitative behaviour was demonstrated to be wrong. It is worth noting that these models can predict values that stay in the range of the actual measurements despite a very small increase (instead of the observed decrease), see Figures 6, so that the simulation does not appear to be quantitatively aberrant.

8. Discussion

From the generic qualitative analysis we have shown that CO_3^{2-} is required in the model to explain the experimental observations. This result can be straightforwardly ex-

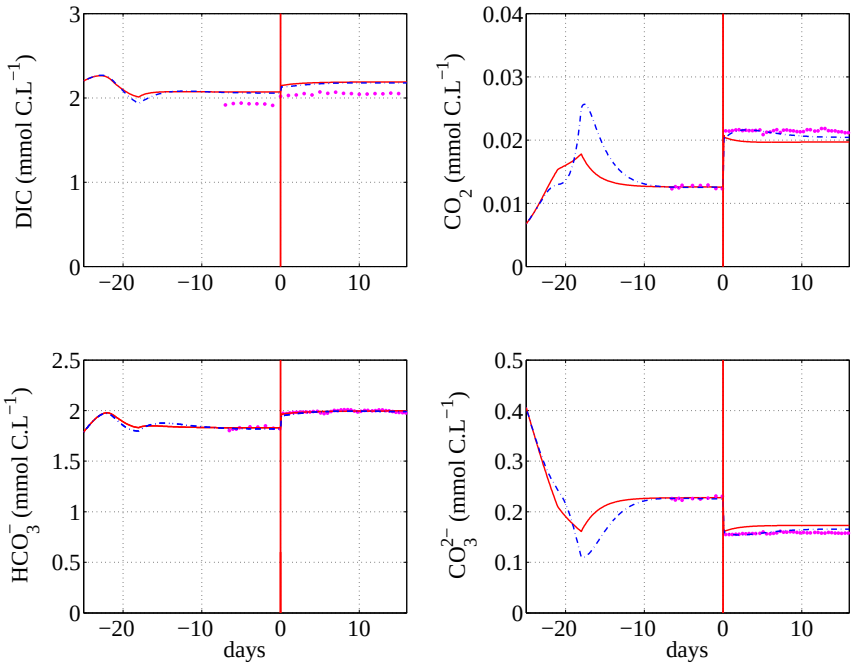

Figure 4. *Comparison between models CI-CO_3^{2-} (—), UI-CO_3^{2-} -HCO_3^- (- · -) and data for the DIC species.*

plained by a simple argument based on the growth rate. We base this reasoning on the assumption that the growth rate (or photosynthesis rate) is an increasing function of both the internal quota and a controlling inorganic carbon compound. The experimentally observed biomass decrease induced by the shift of pCO_2 leads to an increase in the internal quota (since particulate nitrogen stays constant). Now if we keep in mind that, under chemostat steady state, the growth rate is constant (and equals the dilution rate d), this implies that the increase in internal quota must be compensated by a decrease of the controlling variable in order to maintain a constant growth rate. The only variable to decrease in response to the shift in the bicarbonate system is CO_3^{2-}. It therefore explains why only this model can provide an adequation with the experiments.

The multimodel analysis therefore leads to the conclusion that, in the model, CO_3^{2-} must be implicated in the photosynthesis regulation. This conclusion is surprising and is not clearly supported by any experimental evidence. In fact, these unexpected conclusions have already been obtained in a previous study implying a simpler Monod based growth model depending directly from external nitrate and from an inorganic carbon species. Since such models did not lead to the expected consistency between observation and process knowledge, we progressively complexified the model to make it closer to biology, but the changes did not affect the conclusion. This was also why the expressions have been considered generic, so as to make sure that the conclusions were not dependent on a specific form chosen for the photosynthesis or calcification rates.

The main conclusion of our study is that CO_3^{2-} may play a key role for coccolithophores. This hypothesis has been also raised in a recent paper [11], where the authors

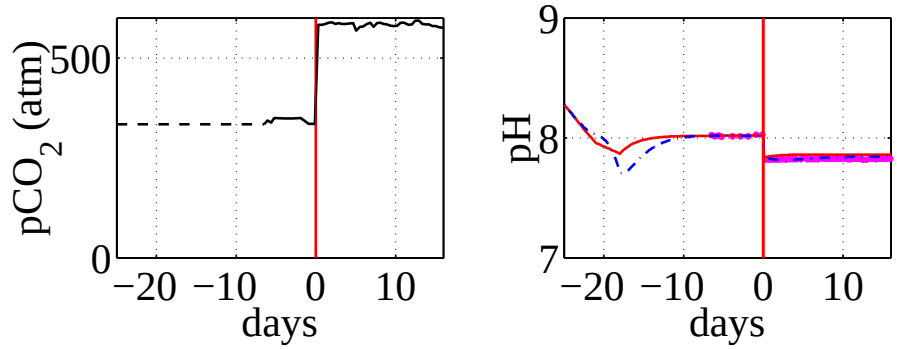

Figure 5. *pCO_2 evolution in the chemostat and comparison between models CI-CO_3^{2-} (—), UI-CO_3^{2-} -HCO_3^- (- · -) and data for pH.*

state that the condition of high CO_3^{2-} can be considered a crucial ecological factor for the success of *E. huxleyi*.

We have shown that a quantitative approach would have been misleading. If we had developed a single model on the basis of the classical hypotheses (model UI-CO_2 -HCO_3^-), we would have end up with a calibration procedure minimising the prediction error. Figure 6 would have inexorably lead to a sentence like ”the graph demonstrates a good adequation between model and data” which would have justified the use of model UI-CO_2 -HCO_3^- . Developing a theory on the basis of the model allows to draw conclusions that are independent of parameter values and even on the precise functions used in the model. As a consequence we end-up with a more objective and fruitfull information to test the model. We have also shown that this approach can drive the experimentalist toward experiments that can critically distinguish models and eliminate inappropriate models (see also [15]). Here a better measurement of C/X would be decisive to identify the more appropriate model.

Finally, our qualitative approach has stimulated a multi model development. We strongly recommend this point of view where the model designer is not the ”owner” of a specific model. Considering models in parallel provides more freedom to criticise a model and finally reject it. This is often difficult when the model under study was the result of several years of investments.

9. Conclusion

We have developed a multimodel generic approach to investigate the coupled effect of a nitrogen limitation and of a pCO_2 increase. We have proposed 12 models of the production and calcification rates of *E.huxleyi* based on several possible regulation mechanisms. These models are generic since they only rely on qualitative hypotheses. The only possible set of models that can explain both a decrease of calcification and of photosynthesis are those where photosynthesis is regulated by CO_3^{2-} . This is not supported by classical hypotheses, even if they were stated on the basis of nitrogen unlimited cultures. However this conclusion is consistent with [11] who state that the condition of high CO_3^{2-} can be considered a crucial ecological factor for the success of *E. huxleyi*.

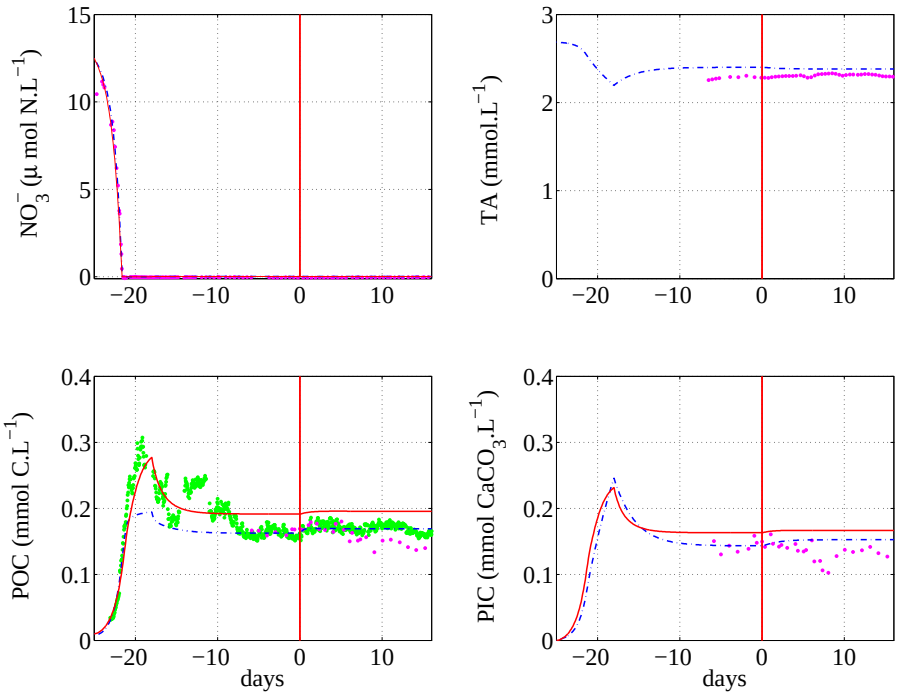

Figure 6. *Comparison between models CI-HCO_3^- (—), UI-CO_2 -HCO_3^- (- · -) and data for POC (X), PIC (C) Nitrate (S_1) and TA. Organic carbon is simultaneously estimated by biovolume (light grey points)*

Finally we show that our conclusions could not have been obtained with a ”classical” quantitative approach. In such a study we would probably have developed a model based on standard assumptions that would have produced (on our experimental data set) a ”good adequation with experimental data”.

Acknowledgements: Funding was provided by the BOOM project (Biodiversity of Open Ocean Microcalcifiers) supported by the French National Research Agency (ANR).

APPENDIX A: pH computation considering borate effect

Let us denote by B_T the total Bohr concentration, the contribution of borate to alkalinity is therefore:

$$\lambda_0 = \frac{K_B}{K_B + h} B_T$$

We can thus compute the fraction $r = \frac{D}{CA} = \frac{h+K_2+h^2/K_1}{h+2K_2}$, and we get:

$$\frac{h + K_2 + h^2/K_1}{h + 2K_2} - \frac{D}{\lambda + 2S_2 - \frac{K_B}{K_B+h} B_T + h - K_{H_2O}/h} = 0$$

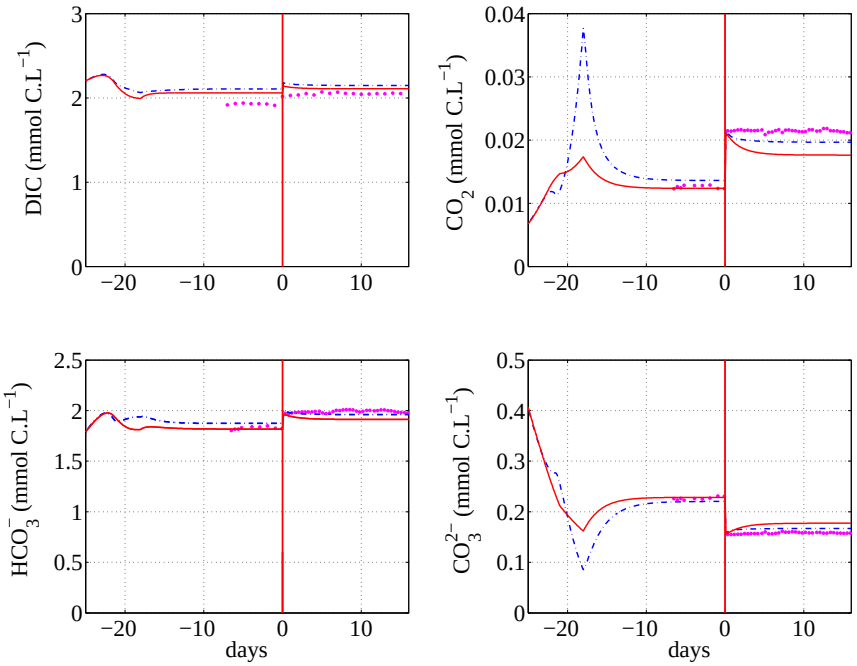

Figure 7. *Comparison between models CI-HCO_3^- (—), UI-CO_2 -HCO_3^- (- · -) and data for the DIC species.*

Knowing S_2, D and λ this provides the 4th order polynomial equation for h that must be solved. In practice this equation is solved as a minimisation problem initialised with the solution provided by equation (11).

This more accurate computation provides however results very close to one obtained with equation (11).

APPENDIX B: proof of Property 4

1- let us first assume that $Dp = Dc$. Equation (59) where ω and σ are both increasing, straightforwardly demonstrates that $\frac{\partial S_2^*}{\partial Dc^*} < 0$.

If $Dc = CO_2$ it directly gives $\frac{\partial S_2^*}{\partial CO_2^*} < 0$.

If $Dc = CO_3^{2-}$, since CO_2 is an increasing function of S_2 and a decreasing function of CO_3^{2-} : $CO_2 = \psi_{CO_2-CO_3^{2-}}(CO_3^{2-}, S_2)$, we have

$$\frac{\partial CO_2^*}{\partial S_2^*} = \frac{\partial \psi_{CO_2-CO_3^{2-}}}{\partial Dc}\frac{\partial Dc}{\partial S_2} + \frac{\partial \psi_{CO_2-CO_3^{2-}}}{\partial S_2^*} > 0$$

Finally when $Dc = HCO_3^-$, since $\psi_{CO_2-HCO_3^-}$ is an increasing function of HCO_3^- and a decreasing function of S_2, it gives $\frac{\partial CO_2^*}{\partial S_2^*} < 0$.

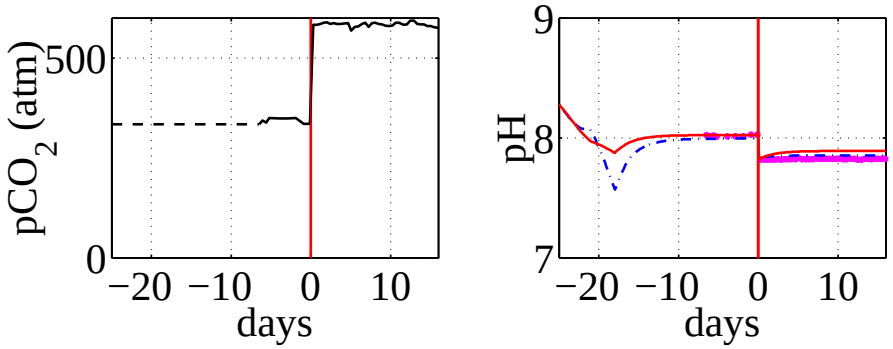

Figure 8. *Applied pCO_2 and comparison between models CI-HCO_3^- (—), UI-CO_2 - HCO_3^- (- · -) and data for pH.*

To conclude the proof, D can be expressed as an increasing function of S_2 and CO_2 , which leads to:

$$\frac{\partial D}{\partial CO_2} = \frac{\partial \psi}{\partial CO_2} + \frac{\partial \psi}{\partial S_2}\frac{\partial S_2}{\partial CO_2}$$

For the cases where $\frac{\partial S_2}{\partial CO_2} > 0$, we get directly $\frac{\partial D}{\partial CO_2} > 0$, in the other cases a numerical computation shows that this result is always true.

2- In order to simplify the notations let us denote by ψ_{cp} the function relating Dc^* to S_2^* and Dp^* : $Dc^* = \psi_{cp}(Dp^*, S_2^*)$

Now we can differentiate this expression with respect to Dp^*:

$$\frac{\partial Dc^*}{\partial Dp^*} = \frac{\partial \psi_{cp}}{\partial Dp^*} + \frac{\partial \psi_{cp}}{\partial S_2^*}\frac{\partial S_2^*}{\partial Dp^*} \tag{61}$$

The term $\frac{\partial S_2}{\partial Dp^*}$ can be computed using expression (59):

$$\frac{\partial S_2}{\partial Dp^*} = -\frac{1}{d}\omega'(Dp^*)\sigma(Dc^*) - \frac{1}{d}X^*\sigma'(Dc^*)\frac{\partial Dc}{\partial Dp} \tag{62}$$

Combining this expression with equation (61) it gives:

$$\frac{\partial S_2}{\partial Dp^*}\left[1 + \frac{1}{d}X^*\sigma'(Dc^*)\frac{\partial \psi_{cp}}{\partial S_2}\right] = -\frac{1}{d}\omega'(Dp^*)\sigma(Dc^*) - \frac{\sigma'(Dc^*)X^*}{d}\frac{\partial \psi_{cp}}{\partial Dp} \tag{63}$$

and

$$\frac{\partial Dc^*}{\partial Dp^*}\left[1 + \frac{\sigma'(Dc)X^*}{d}\frac{\partial \psi_{cp}}{\partial S_2}\right] = -\frac{\partial \psi_{cp}}{\partial S_2}\frac{\sigma(Dc)\omega'(Dp)}{d} + \frac{\partial \psi_{cp}}{\partial Dp} \tag{64}$$

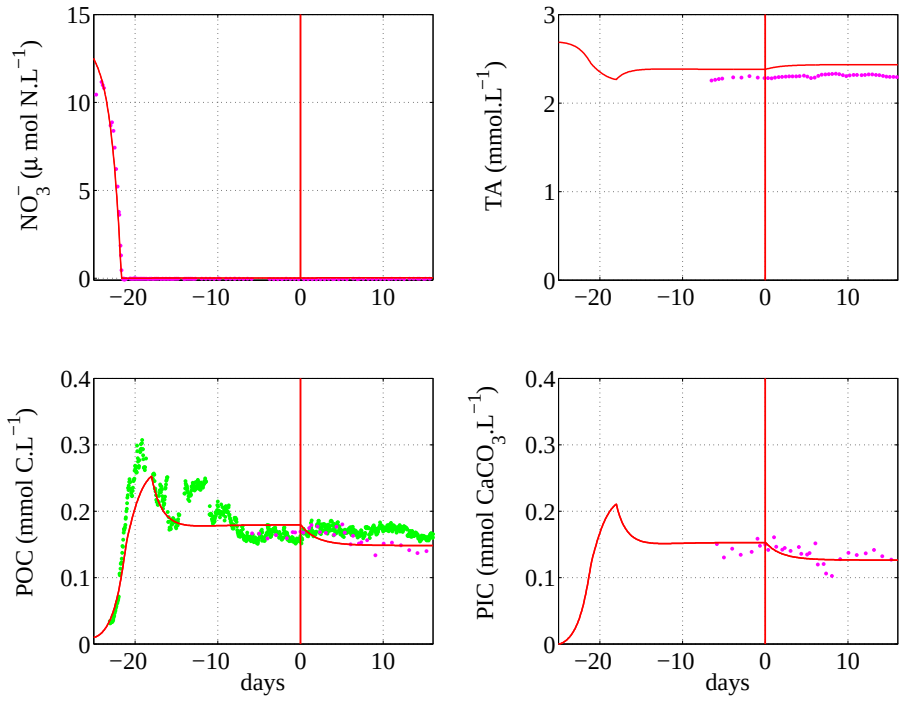

Figure 9. *Comparison between model CI-pH (—), and data for POC (X), PIC (C) Nitrate (S_1) and TA. Organic carbon is simultaneously estimated by biovolume (light grey points)*

To conclude we need to study the signs of the quantities defined as follows:

$$A_1 = \frac{\partial \psi_{cp}}{\partial S_2} \frac{\sigma'(Dc) X^*}{d} \text{ , } A_2 = X^* \sigma'(Dc^*) \frac{\partial \psi_{cp}}{\partial Dp} \text{ , } B_1 = A_2/(\sigma(Dc^*)\omega'(Dp^*))$$

and $B_2 = -\frac{\partial \psi_{cp}}{\partial S_2} / \frac{\partial \psi_{cp}}{\partial Dp} \frac{\sigma(Dc^*)\omega'(Dp^*)}{d}$.

Note that the signs of A_1, A_2, B_1 and B_2 are directly related to the partial derivatives of ψ_{cp}.

Table 3 summarises the signs of A_1, A_2 and B_1 associated to each model. In the cases where it is not possible to conclude directly from generic arguments, quantities A_1, A_2 or B_1 are computed assuming a $\pm 10\%$ variation of the parameters (200 different combinations of parameter values are considered) and the ranges of variations are provided.

For example, in the case when Dc or Dp is CO_3^{2-} , $Dc = \psi_{cp}(Dp, S_2)$ is an increasing function of S_2 and a decreasing function of Dp. As a consequence (63) shows that A_1 is positive and that the sign of $\frac{\partial S_2}{\partial Dp^*}$ is determined by the term $-A_2(1 + 1/B_1)$, whose sign is *a priori* unknown.

A numerical study of the ratio B_1, considering various parameter values allows to determine which term dominates in the sum.

In this case it is worth noting that $CO_2 = \frac{K_1}{K_2} \frac{(HCO_3^-)^2}{CO_3^{2-}}$ is an increasing function of HCO_3^- and a decreasing function of CO_3^{2-} , which proves that $\frac{\partial CO_2^*}{\partial CO_3^{2-*}} < 0$

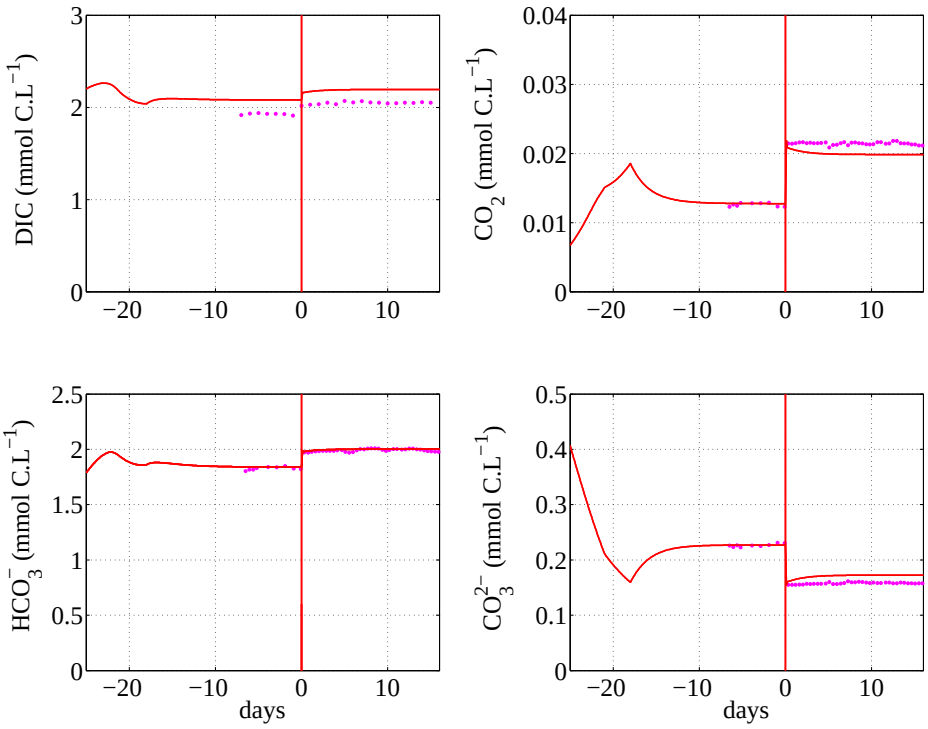

Figure 10. *Comparison between model CI-pH and data for the DIC species.*

Now in the remaining cases where Dc orDp is CO_2 , ψ_{cp} is an increasing function of HCO_3^- , so that the right hand side of equation (63) is positive. When Dc is CO_2 a numerical computation is required since $A_1 < 0$. When Dp is CO_2 , $A_1 > 0$ and $B_1 > 0$ such that R_2 must be numerically evaluated (see Table 3) to determine the sign of $\frac{\partial Dc^*}{\partial Dp^*}$.

10. References

[1] G. BASTIN and D. DOCHAIN. *On-line estimation and adaptive control of bioreactors*. Elsevier, Amsterdam, 1990.

[2] O. BERNARD, A.SCIANDRA, and S. MADANI. Multimodel analysis of the response of the coccolithophore *Emiliania huxleyi* to an elevation of pCO_2 under nitrate limitation . *Ecol. Model.*, 211:324–338, 2008.

[3] O. BERNARD and G.BASTIN. On the estimation of the pseudo-stoichiometric matrix for mass balance modeling of biotechnological processes. *Math. Biosciences*, 193:51–77, 2005.

[4] D. E. BURMASTER. The unsteady continuous culture of phosphate-limited *Monochrysis lutheri* Droop: experimental and theoritical analysis. *J. Exp. Mar. Biol. Ecol.*, 39(2):167–186, 1979.

[5] M. R. DROOP. Vitamin B12 and marine ecology. IV. the kinetics of uptake growth and inhibition in *Monochrysis lutheri*. *J. Mar. Biol. Assoc.*, 48(3):689–733, 1968.

[6] M. R. DROOP. 25 years of algal growth kinetics, a personal view. *Botanica marina*, 16:99–112, 1983.

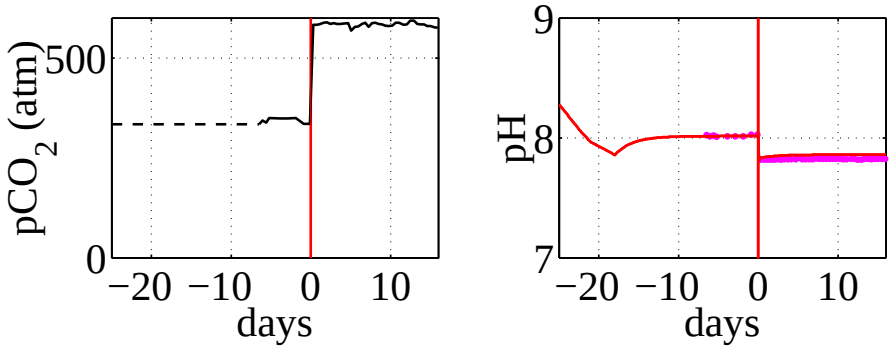

Figure 11. *Applied pCO_2 and comparison between model CI-pH and data for pH.*

[7] R. C. DUGDALE. Nutrient limitation in the sea: dynamics, identifi cation and signifi cance. *Limnol. Oceanogr.*, 12:685–695, 1967.

[8] P. G. FALKOWSKI. Evolution of the nitrogen cycle and its influence on the biological sequestration of co2 in the ocean. *Nature*, 327:242–244, 1997.

[9] M. FRANKIGNOULLE, C. CANON, and J. P. GATTUSO. Marine calcifi cation as a source of carbon dioxide: positive feedback of increasing atmospheric co2. *Limnol Oceanogr*, 39:458–462, 1994.

[10] J. T. HOUGHTON, JENKINS G. J., and EPHTRAIMS J. J. *Climate Change 1995, The Science of Climate Change*. Cambridge University Press, 1996.

[11] A. MERICO, T. TYRRELL, and T. COKACAR. Is there any relationship between phytoplankton seasonal dynamics and the carbonate system? *J. Mar. Syst.* , 59:120–142, 2006.

[12] E. PAASCHE. A review of the coccolithophorid *emiliania huxleyi* (prymnesiophyceae), with particular reference to growth, coccolith formation, and calcifi cation-photosynthesis interaction. *Phycologia*, 40:503–529, 2002.

[13] U. RIEBESELL, I. ZONDERVAN, B. ROST, P.D. TORTELL, R. E. ZEEBE, and F. M. M. MOREL. Reduced calcifi cation of marine plankton in response to increased atmospheric co2. *Nature*, 407:364–367, 2000.

[14] A. SCIANDRA, J. HARLAY, D. LEFÈVRE, R. LEMÉE, P. RIMMELIN, M. DENIS, and J.-P. GATTUSO. Response of coccolithophorid *emiliania huxleyi* to elevated partial pressure of co2 under nitrogen limitation. *Mar. Ecol. Prog. Ser.*, 261:111–122, 2003.

[15] I. VATCHEVA, H. DEJONG, O. BERNARD, and N.J.L. MARS. Experiment selection for the discrimination of semi-quantitative models of dynamical systems. *Artif. Intel.*, 170, 2006.

[16] R. E. ZEEBE and D. WOLF-GLADROW. *CO_2 in seawater: equilibrium, kinetics, isotopes*. Elsevier, 2003.

[17] I. ZONDERVAN, B. ROST, and U. RIEBESELL. Effect of co2 concentration on the pic/poc ratio in the coccolithophore *emiliania huxleyi* grown under light-limiting conditions and different daylengths. *J Exp Mar Biol Ecol*, 272:55–70, 2002.